Available online at www.sciencedirect.com
ScienceDirect
Journal of Solid State Chemistry 180 (2007) 2026–2033
JOURNAL OF SOLID STATE CHEMISTRY
www.elsevier.com/locate/jssc

Nb–Ta, Nb–Mo and Nb–V oxides prepared from hybrid organic–inorganic precursors

N. Deligne, D. Bayot, M. Degand, M. Devillers*

Unité de Chimie des Matériaux Inorganiques et Organiques, Université Catholique de Louvain, Place Louis Pasteur 1, B-1348 Louvain-la-Neuve, Belgium

Received 17 January 2007; received in revised form 4 May 2007; accepted 6 May 2007
Available online 18 May 2007

Abstract

New hybrid organic–inorganic materials based on group 5 elements and a well-defined polymeric matrix have been prepared and used as precursors for Nb–Ta and Nb–Mo mixed oxides. In this non-conventional but easily accessible route to multimetallic oxides, a copolymer of *N*,*N*-diallyl-*N*-hexylamine and maleic acid was synthesised and used as matrix to stabilise inorganic species generated in solution from $(NH_4)_6Mo_7O_{24}\cdot 4H_2O$, NH_4VO_3, $(gu)_3[Nb(O_2)_4]$ and $(gu)_3[Ta(O_2)_4]$. Solid-state studies indicate that the homogeneity of the blends can be kept up to about 0.5 mol Nb^V and Ta^V and 0.25 mol V^V per mol of repeat units of the copolymer. The calcination conditions of these homogeneous hybrid precursors were optimised to produce Nb–Mo, Nb–Ta and Nb–V oxides. While the thermal treatment of the Nb–V hybrid blends led only to a mixture of different phases, the characterisation of the final phases by X-ray diffraction (XRD) proved the formation of pure $Nb_2Mo_3O_{14}$ and showed that Nb–Ta oxides could be synthesised as single phases corresponding to a continuous series of solid solutions.

Keywords: Niobium; Tantalum; Molybdenum; Vanadium; Precursors; Hybrid materials; Mixed oxides

1. Introduction

Multimetallic oxides based on group 5 elements generate a great interest because of their attractive physical properties. For instance, Nb-based oxides are widely studied as ferroelectric and piezoelectric materials such as $BiNbO_4$ [1], or as fast ion conductors such as Y_3NbO_7 [2]. Moreover, a large number of oxides based on group 5 elements are known to exhibit catalytic activities in several highly challenging industrial processes. Whereas niobium pentoxide itself is a very selective but poorly active catalyst for propane oxidative dehydrogenation [3], its association with some more easily reducible elements such as V and Mo improves the catalytic activity while maintaining a high selectivity [4]. In that context, the mixed oxides $NbVO_5$ and $Nb_2Mo_3O_{14}$ are of particular interest but are rather difficult to produce by conventional synthesis routes. In addition, some mixed oxides based on Nb^V and Ta^V, like the solid solutions $(Nb_{1-x}Ta_x)_2O_5$ and $Nb_{1-x}Ta_xBiO_4$, are reported as efficient catalysts for water photodecomposition [5,6].

Multicomponent oxides are classically prepared via standard procedures such as the conventional solid-state reaction. This method was successfully implemented for the preparation of $Nb_2Mo_3O_{14}$ but the reaction needs to be carried out in sealed vials in order to avoid sublimation of MoO_3 [7,8]. $(Nb_{1-x}Ta_x)_2O_5$ oxides have also been prepared from simple oxides and a phase diagram was established in the high-temperature range by Mohanty et al. [9]. Unfortunately, such methods lead in most cases to poorly homogeneous materials and to large particles due to the high temperatures used. Some alternative methods based on precursors are also extensively used such as the well-known sol–gel and citrate routes [10]. For instance, $(Nb_{1-x}Ta_x)_2O_5$ solid solutions have been prepared by a neutral templating sol–gel route, using the pentachlorides as metal precursors and a block copolymer as template [11]. Recently, the mixed oxides $Nb_2Mo_3O_{14}$ and $(Nb_{1-x}Ta_x)_2O_5$ have also been prepared by a molecular

*Corresponding author. Fax: +32 10/472330.
E-mail address: devillers@chim.ucl.ac.be (M. Devillers).

0022-4596/$ - see front matter © 2007 Elsevier Inc. All rights reserved.
doi:10.1016/j.jssc.2007.05.008

precursor route based on the decomposition of carboxylates and polyaminocarboxylates complexes [12,13]. All these precursors routes exhibit different advantages, mainly the implementation of rather soft temperatures to produce the oxides and an increased homogeneity of the final product. According to these procedures, it is usually possible to prepare bulk or dispersed mixed oxides exhibiting well-defined characteristics with respect to stoichiometry, structure, specific surface area and morphology.

A few years ago, an original approach towards the synthesis of multicomponent oxides, based on hybrid organic–inorganic materials, has been developed in our laboratory. In this method, inorganic salts are incorporated into a polyzwitterionic matrix—namely a polymer bearing cationic as well as anionic moieties—to give homogeneous hybrid blends which are isolated at the solid state. The presence, at the same time, of positively and negatively charged moieties in the structure of the polymer matrix makes it suitable to stabilise and interact with both anions and cations. Under certain pH and concentration conditions, amorphous hybrid organic–inorganic materials can be obtained and can be further used as precursors of inorganic materials. Within that context, poly(sulphobetaine)s and poly(carbobetaine)s were used to prepare hybrid blends from simple inorganic salts such as NaBr, NaI and $LiClO_4$ [14–16]. Additionally, some transition metals were also successfully incorporated in poly(sulphobetaine)s matrices [17]. More recently, we reported the association of some poly(carbobetaine)s matrices with a number of transition metals, namely Ni^{III}, Co^{III}, V^{V} and Mo^{VI}. A final thermal treatment of these hybrid precursors has allowed the production of nickel, cobalt and manganese molybdates as well as bismuth vanadates at relatively moderate temperatures [18–20]. For instance, it was possible to stabilise the metastable γ-$Bi_4V_2O_{11}$ phase at an unexpected temperature of 300 °C [19]. In addition, the sacrificial matrices used were shown to exhibit a low final decomposition temperature and, because they are free of heteroatoms such as S, P or halogens, very high levels of chemical purity can be attained for the final material. In some selected cases, elemental analysis was carried out on the final oxides and demonstrated a residual carbon content well below 0.3%, and no nitrogen contamination at all [18,19].

The purpose of this work is to extend the applicability of the hybrid organic–inorganic precursors method for the preparation of oxide phases containing group 5 elements. A well-defined polymeric matrix was therefore synthesised by copolymerisation of a diallylamine derivative and maleic acid following an already described synthesis route [21]. Niobium^{V}, tantalum^{V}, vanadium^{V} and molybdenum^{VI} were then incorporated in this matrix and the homogeneity of the samples was checked in solution as well as in the solid state. In addition, we were also interested in the investigation of the interactions between the metal species and the polymer. Finally, homogeneous hybrid materials containing two different metallic species were used for the synthesis of multimetallic oxides, namely $(Nb_{1-x}Ta_x)_2O_5$ and $Nb_2Mo_3O_{14}$ and the required conditions to produce these oxides were investigated and optimised.

2. Experimental

2.1. Materials/solvents

Solvents used, namely methanol (Fluka Chemika), ethanol (Fischer Scientific) and dichloromethane (Fluka Chemika), were analytical reagent grade. Maleic acid, *N*,*N*-diallylamine and guanidinium carbonate $(gu)_2CO_3$ were purchased from Aldrich. 1-Bromohexane, ammonium heptamolybdate tetrahydrate $(NH_4)_6Mo_7O_{24}\cdot 4H_2O$, ammonium metavanadate NH_4VO_3, hydrogen peroxide H_2O_2 (35 wt%) and ammonia (25%) were supplied from Acros. Tantalum pentachloride, $TaCl_5$, was purchased from Alfa Aesar. Niobic acid was supplied from CBMM, Brazil. 2,2′-azobis [2-methyl-*N*-[1,1-bis(hydroxymethyl)-2-hydroxyethyl] propionamide] (VA086) was purchased from Wako. Water used during polymer synthesis and purification steps was first purified using an Elgastat Maxima system (resistance: 18.2 mΩ). Spectra/Por dialysis membranes (nominal cut-off: 2000 Da) and a strongly acidic exchange resin (Amberlite IR-120) were employed for polymer purification. All reagents were of analytical grade and used without further purification.

2.2. Methods

Monomer ^{13}C spectra were taken on a Bruker 300 MHz Ultrashield™ spectrometer. Polymer ^{13}C-NMR experiments were performed on a 500 MHz spectrometer (Bruker, Avance 500). ^{13}C chemical shifts were calibrated to the residual signals of the solvent for $CDCl_3$. For the calibration of ^{13}C shifts in D_2O, sodium 2,2-dimethyl-2-silapentane-5-sulphonate (DSS, Aldrich) was employed as an external reference. Elemental analysis was carried out at University College, London, UK. Thermogravimetric analyses (TGAs) were carried out under flowing air (100 mL min^{-1}) on a Mettler Toledo 851^{e} thermogravimetric analyser, applying a heating rate of 10 °C min^{-1}. Powder X-ray diffraction (XRD) data were collected on a Siemens D5000 diffractometer, using the Cu$K\alpha$ line ($\lambda = 0.15418$ nm). FT-Raman spectra were taken on a Bruker RFS100/S spectrometer, at a wavelength of 1064 nm. Scanning electron microscopy (SEM) was performed with a Gemini Digital Scanning Microscope 982 with 1 kV accelerating voltage. X-ray photoelectron spectroscopy (XPS) measurements were carried out at room temperature on an SSI-X-probe (SSX-100/206) photoelectron spectrometer from FISONS using the Al$K\alpha$ radiation ($E = 1486.6$ eV) and a sample holder. Charge effects were avoided by placing a nickel grid above the samples and using a flood gun set at 8 eV. The energy scale was calibrated with reference to the Au4$f_{7/2}$ peak at 84 eV,

and the binding energies were calculated with respect to the C–(C,H) component of the C 1*s* peak fixed at 284.8 eV. The area ratio $A(\text{Mo } 3d_{5/2})/A(\text{Mo } 3d_{3/2})$ was fixed at 1.50, and the difference in binding energy between the two components of the Mo 3*d* doublet was fixed at 3.13 eV.

2.3. Monomer and polymer syntheses

The model copolymer selected in this work is made from the association of *N*,*N*-diallyl-*N*-hexylamine and maleic acid, according to Fig. 1.

2.3.1. *N,N-diallyl-N-hexylamine* (**1**)

The monomer was synthesised according to a synthesis pathway described elsewhere [21]. ^{13}C-NMR (75 MHz, $CDCl_3$): δ (ppm) = 135.7 (–CH =), 117.2 (= CH_2), 56.8 (–N–*C*H_2–C =), 53.4 (–N–CH_2–alkyl), 31.8 (–*C*H_2–CH_2–CH_3), 27.1 (–N–CH_2–*C*H_2–), 26.8 (N–CH_2–CH_2–*C*H_2–), 22.6 (–*C*H_2–CH_3) 14.0 (–CH_3). Elem. Anal. Calcd. for $C_{12}H_{23}N$ (M = 181.32): C, 79.49; H, 12.79; N, 7.72; Found: C, 77.96; H, 12.64; N, 7.60.

2.3.2. *Poly(N,N-diallyl-N-hexylamine-co-maleic acid)* (**2**)

The synthesis of the polymer matrix has been published in a previous paper [21]. ^{13}C-NMR (125 MHz, D_2O, 80 °C, sodium salt): δ (ppm) = 182.2 (COOH), 58.6, 57.6 and 57.0 (N–CH_2–), 53.0, 52.1 and 51.3 (–*C*H–C(= O)), 40.6 and 39.2 (N–C–*C*H–), 42.8, 31.5, 26.4 and 26.0 (C(= O)–C–*C*H_2 and N–C–*C*H_2–*C*H_2–*C*H_2–), 22.6 (–*C*H_2–CH_3), 14.2 (–CH_3). Elem. Anal. Calcd. for $C_{16}H_{27}NO_4$ (M = 297.39): C, 64.62; H, 9.15; N, 4.71; C/N ratio, 13.72; Found: C, 61.22; H, 9.38; N, 4.56; C/N ratio, 13.43.

2.4. Niobium^{v} and tantalum^{v} derivatives

The lack of commercially available water-soluble Nb^V and Ta^V compounds has justified some previous work to isolate appropriate coordination compounds that can be used as precursors. In particular, we described recently some new peroxo-type Nb^V and Ta^V derivatives [22,23]. In this present work, $(gu)_3[Nb(O_2)_4]$ and $(gu)_3[Ta(O_2)_4]$ were used as starting materials for the preparation of the hybrid blends. Their synthesis consists of the reaction between niobic or tantalic acid and guanidinium carbonate in the presence of an excess of hydrogen peroxide. $(gu)_3[Nb(O_2)_4]$ Elem. Anal. Calcd. for $C_3H_{18}N_9O_8Nb$ (M = 401.14): C, 8.98; H, 4.52; N, 31.42; Found: ,C, 8.88; H, 4.57; N, 30.71. $(gu)_3[Ta(O_2)_4]$ Elem. Anal. Calcd. for $C_3H_{18}N_9O_8Ta$ (M = 489.18): C, 7.37; H, 3.71; N, 25.77; Found: C, 7.63; H, 3.68; N, 25.22.

2.5. Preparation of the hybrid materials

In a typical experiment, the polymer was dissolved in distilled water to give a 0.02 mol L^{-1} solution. The appropriate amounts of 0.01 mol L^{-1} aqueous solutions of the inorganic species, namely $(NH_4)_6Mo_7O_{24}\cdot 4H_2O$, NH_4VO_3, $(gu)_3[Nb(O_2)_4]$ or/and $(gu)_3[Ta(O_2)_4]$, were added in order to reach the desired molar ratio of metal ion(s) per repeat unit of copolymer. The pH value was adjusted to a value of 10 by means of 0.1 mol L^{-1} aqueous NH_3. The solution was stirred at room temperature for 30 min and then freeze-dried to give a finely divided powder.

2.6. Preparation of the oxides

Hybrid materials containing Nb^V and/or Ta^V were calcined at 700 °C for 2 h in air. According to this method, different oxides with the general formula $(Nb_{1-x}Ta_x)_2O_5$ were prepared with various compositions, namely for x = 0, 0.25, 0.5, 0.75 and 1. Homogeneous organic–inorganic materials containing Nb^V and Mo^{VI} in a molar ratio Nb/Mo of 2/3 were calcined in air at temperatures of 600, 650 and 700 °C. In one case, a first calcination step at 350 °C for 2 h was carried out and was followed by firing at 700 °C for another 2 h. Hybrid materials containing 0.25 mol Nb^V and 0.25 mol V^V per mol of repeat unit of copolymer were annealed at 500 and 600 °C for 3 h.

3. Results and discussion

3.1. Solution and solid-state studies of the precursors

The miscibility of the polymer matrix with the inorganic salts was first screened for different molar ratios of salt relatively to the repeat unit of the copolymer. The homogeneity of the solutions was checked by a naked-eye qualitative appreciation of their transparency. The results

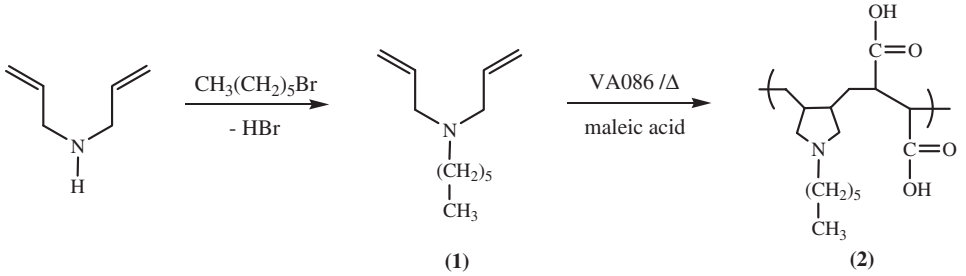

Fig. 1. Facile synthetic route to the precursor monomer and copolymer matrix.

indicate that all the samples prepared are homogeneous in solution. After freeze-drying, the hybrid blends were analysed by powder XRD measurements. As illustrated in Fig. 2, in some cases, sharp lines appear in the diffractograms, suggesting that a part of the inorganic species does not interact with the matrix and forms a separate crystalline phase. Such a behaviour has been observed previously on similar systems [18]. In such cases, the hybrid blends are considered as inhomogeneous at the solid state. Some test samples were prepared by mixing and grinding in the solid state the polymer with each of the inorganic salts with a molar ratio of 0.1 mol of metal per mol of repeat unit of copolymer. The presence of sharp lines in the diffractograms indicated clearly the presence of a crystalline phase due to the inorganic species. Table 1 summarises the results obtained for the hybrid blends containing only one type of metal. The polymer matrix used allowed the preparation of homogeneously mixed amorphous precursors containing up to 0.5 mol Nb^V and Ta^V and only 0.25 mol V^V per mol of repeat unit of copolymer. The behaviour of Mo-based hybrid blends was already described elsewhere [20]. In addition, Raman spectroscopy was implemented in order to study the nature of the interaction between the metal species and the matrix,

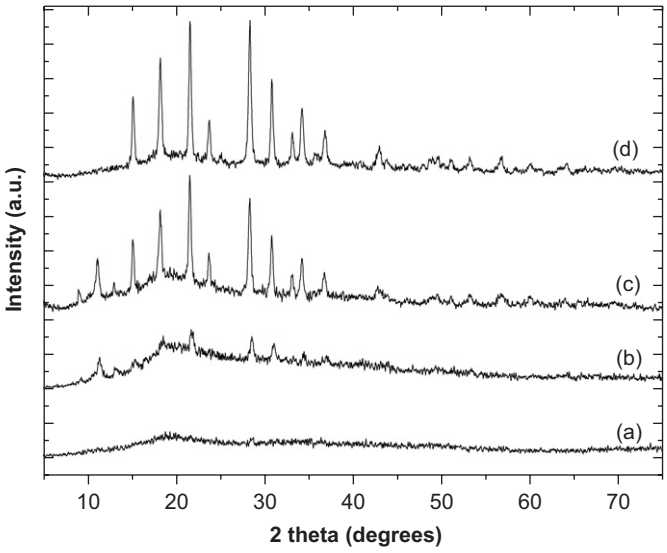

Fig. 2. X-ray diffraction patterns for hybrid materials containing 0.25 (a), 0.5 (b), 1 (c) and 2 (d) mol V^V per mol of repeat unit of copolymer.

Table 1
Screening of the homogeneity of the hybrid blends prepared by incorporation of different amounts of Nb, Ta and V salts in the polymer matrix

Moles of metal per mole of repeat unit of copolymer	0.25	0.5	1	2
$gu_3[Nb(O_2)_4]$	V	V	X	X
$gu_3[Ta(O_2)_4]$	V	V	X	X
NH_4VO_3	V	X	X	X

V, homogeneous material; X, inhomogeneous material.

and namely to look whether coordination bonds take place between the metal and the carboxylate and/or the amine moieties. Such interactions are expected to shift slightly the Raman peaks associated to the metal species and the coordinating moiety. Raman spectra of hybrid blends based on all the metal compounds were therefore taken for various molar ratios of metal relatively to the copolymer repeat unit. However, no significant shift of the bands was observed whatever the metal and the molar ratio. These results are in agreement with a previous work showing that the interactions involved are mainly electrostatic [18].

Moreover, hybrid materials containing different kinds of metals in selective molar ratios were also successfully prepared, namely the Nb–Ta system with 0.25 mol of each metal per mol of copolymer repeat unit and the Nb–Mo system with 0.17 and 0.25 mol of metal per mol of copolymer repeat unit, respectively.

3.2. Thermal behaviour of the precursors

The thermal decomposition of the precursors synthesised from NH_4VO_3, $(gu)_3[Nb(O_2)_4]$ and $(gu)_3[Ta(O_2)_4]$ was followed by TGA as illustrated in Fig. 3. In each TG curve, the first weight loss between 50 and 100 °C is attributed to dehydration. The relatively high quantity of adsorbed water (about 10%) is explained by the hygroscopic character of the polymeric matrix. The TG curves are then composed of several decomposition steps corresponding to the pyrolysis of the organic matrix and the formation of the oxide. The final decomposition temperature lies between 450 and 550 °C which is significantly lower than the final decomposition temperature of the polymer matrix (600 °C). This effect, which was already observed in a previous paper, could be reasonably attributed to the presence of inorganic salts acting as oxidising species [19]. Relating to the Nb^V and Ta^V hybrid blends, a last weight loss of a few percent appears at approximately 580 and 700 °C, respectively. This step is characteristic of niobium and tantalum compounds and its temperature of occurrence remains unchanged whatever the nature of the compound [24]. TG curves of multimetallic hybrid materials were also taken and indicate similar trends. In particular, the TG curve of the organic–inorganic material containing Nb^V and Ta^V (Nb/Ta = 1) exhibits a single last step around 650 °C and does not correspond to a superposition of the TG curves of the hybrid materials based on only one of those two metals. This result suggests a homogeneous distribution of the two metal species in the matrix at the molecular level.

3.3. Characterisation of the final oxides

3.3.1. Nb–Ta–O system

According to the TG analyses, hybrid precursors containing niobium^V and/or tantalum^V salts were calcined at 700 °C for 2 h in air in order to ensure the complete pyrolysis of the organic matrix and the crystallisation of

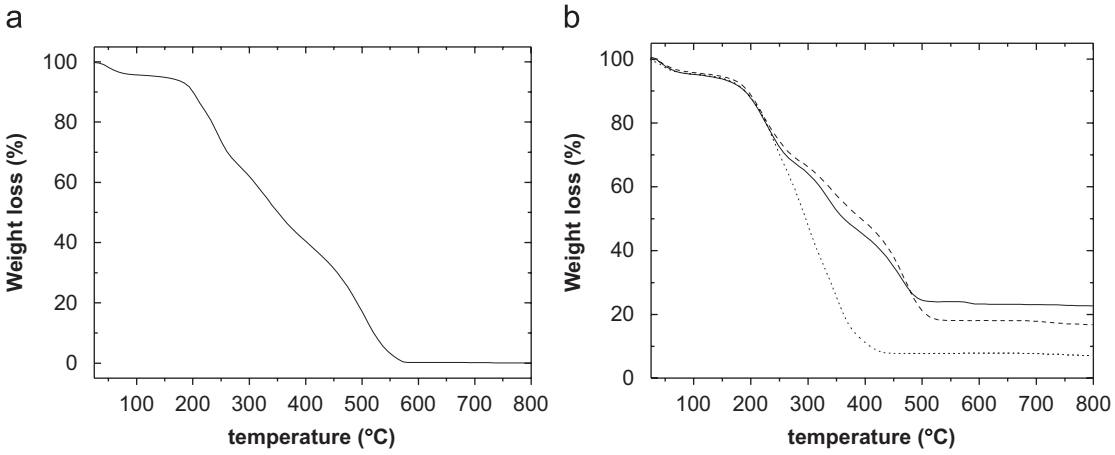

Fig. 3. Thermogravimetric analysis under air of the polymer matrix (a) and of hybrid materials (b) containing 0.5 mol Nb^V (straight line), 0.5 mol Ta^V (dashed line) and 0.25 mol V^V (dotted line) per mol of repeat unit of copolymer.

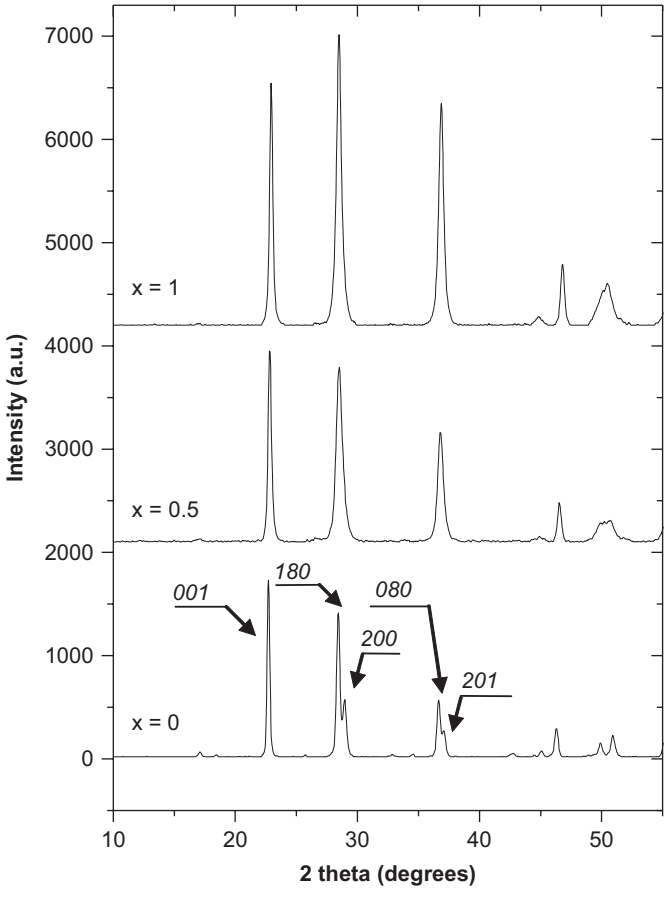

Fig. 4. X-ray diffraction patterns of $(Nb_{1-x}Ta_x)_2O_5$ ($x = 0$, 0.5 and 1).

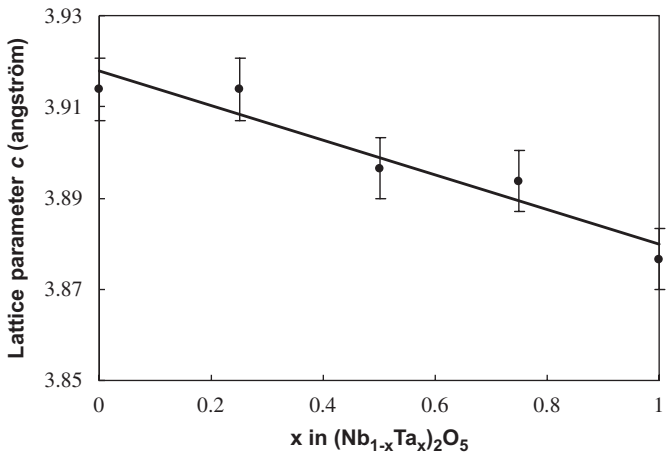

Fig. 5. Evolution of the lattice parameter c as a function of x in $(Nb_{1-x}Ta_x)_2O_5$.

the oxide phases. Fig. 4 illustrates the XRD results obtained for $x = 0$, 0.5 and 1 in $(Nb_{1-x}Ta_x)_2O_5$. All the samples prepared appear to be isostructural with orthorhombic Nb_2O_5 (JCPDS file 30-0873). For several diffraction peaks, slight shifts in 2θ values can be observed between the various compositions. In addition, some overlapping phenomena affect the most intense peaks [13]. For instance, the *180* and *200* reflections are well separated in the XRD pattern of Nb_2O_5 but are too close to each other for the other compositions to be observed as two peaks (Fig. 4). The same observation also holds for the *080* and *201* reflections. The lattice parameter c was calculated from the *001* reflection which appears at a value of 2θ of about 23°. Unfortunately, a and b lattice parameters could not be obtained due to the overlap of the relevant peaks and a too low resolution for the other reflections. Fig. 5 displays the evolution of the parameter c as a function of the composition x. The results put forward a linear decrease of the lattice parameter when the Ta^V content increases. This behaviour follows the Vegard's law and is indicative of the presence of a solid solution in the whole composition domain. A similar behaviour was already observed for the same oxides prepared from molecular precursors based on EDTA and for which c as well as a and b lattice parameters were determined and presented a regular variation when the tantalum content was changed [13].

Additionally, SEM has been used to characterise the morphology of the particles. As shown in Fig. 6, the

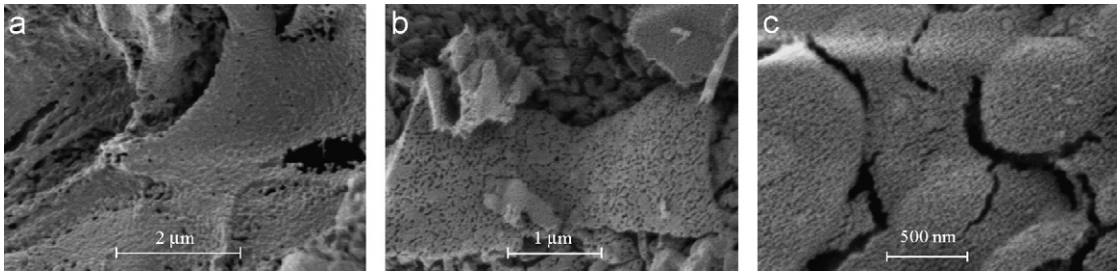

Fig. 6. Typical SEM images of the $(Nb_{1-x}Ta_x)_2O_5$ oxides; $x = 0$ (a), 0.5 (b) and 1 (c).

Nb–Ta oxides exhibit the same morphology whatever the composition x, namely a slight disordered porosity. This is similar to the morphology of Nb–Ta oxides prepared from molecular precursors based on EDTA in a previous work [13].

3.3.2. *Nb–Mo–O system*

Precursors containing Nb^V and Mo^{VI} in a molar ratio Nb/Mo of 2/3 were calcined under various conditions in order to synthesise the mixed oxide $Nb_2Mo_3O_{14}$. Table 2 summarises the different phases obtained as identified by XRD measurements. Calcination at 600 °C during 2 h yields the desired ternary phase (JCPDS file 18-0840) but this procedure does not seem to be relevant to produce the mixed phase in a pure form. Indeed, peaks attributed to the simple oxides, H–Nb_2O_5 (JCPDS file 37-1468) and MoO_3 (JCPDS file 35-0609), appear in the XRD pattern. According to the literature [12], the monoclinic "high temperature" H-Nb_2O_5 is obtained at such a low temperature from the decomposition of the mixed phase $Nb_2Mo_3O_{14}$. A T-form (orthorhombic) would appear if directly occurring from the precursor degradation. Indeed, this mixed oxide is quite unstable once formed and it decomposes quite readily into its corresponding binary oxides, H–Nb_2O_5 and MoO_3, with temperature and time. When the temperature is raised to 650 °C, the desired oxide remains the major phase. However, at this temperature, we observe that the only minor phase is the simple oxide H–Nb_2O_5. This result can be explained by the sublimation of MoO_3 around 700 °C. Finally, a further degradation of the mixed oxide appears when the mixture is fired at a temperature of 700 °C for 2 h. In a previous paper, Nb–Mo oxides were prepared by a molecular precursor route and the decomposition of $Nb_2Mo_3O_{14}$ was described to occur at a higher temperature and after longer calcination time [12]. The results obtained in this work may be explained by a local increase of the temperature in the sample due to the exothermic degradation of the organic matrix. This hypothesis is confirmed by the production of the desired phase in a pure form when a first calcination step is performed at 350 °C, then followed by a further step at 700 °C, as indicated by the XRD pattern (Fig. 7). This first step seems to reduce the total amount of organic material in the sample which reduces the exothermic effect in the second step. The hybrid organic–inorganic method thus allows the formation of the mixed oxide at a temperature lower than that required by the ceramic method, namely 700 °C minimum for its formation and 800 °C to obtain it in a pure form [12], but requires an intermediate firing step at a lower temperature before the final calcination.

Table 2
Different phases obtained upon calcination under various conditions of the hybrid materials based on Nb^V and Mo^{VI} (Nb/Mo = 2/3)

Calcination conditions	$Nb_2Mo_3O_{14}$	MoO_3	H–Nb_2O_5
600 °C/2 h	M	m	m
650 °C/2 h	M	–	m
700 °C/2 h	m	–	M
350 °C/2 h, 700 °C/2 h	M	–	–

M, major phase; m, minor phase.

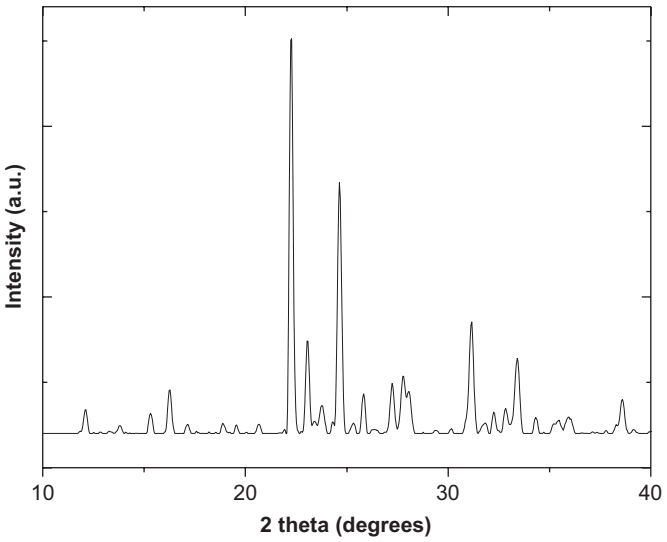

Fig. 7. X-ray diffraction pattern of $Nb_2Mo_3O_{14}$ prepared by calcination of hybrid blends containing Nb^V and Mo^{VI} (Nb/Mo = 2/3; mol/mol) for 2 h at 350 °C then 2 h at 700 °C. All lines correspond to the JCPDS file 18-0840 of the mixed oxide.

Because of the various oxidation states easily accessible for Mo (+IV, +V, +VI), XPS was implemented in order to check for an eventual reduction of this metal during the preparation steps. The Mo *3d* XPS spectrum of the pure $Nb_2Mo_3O_{14}$ phase (Fig. 8) shows that Mo is present in the (+VI) oxidation state only at the surface of the oxide.

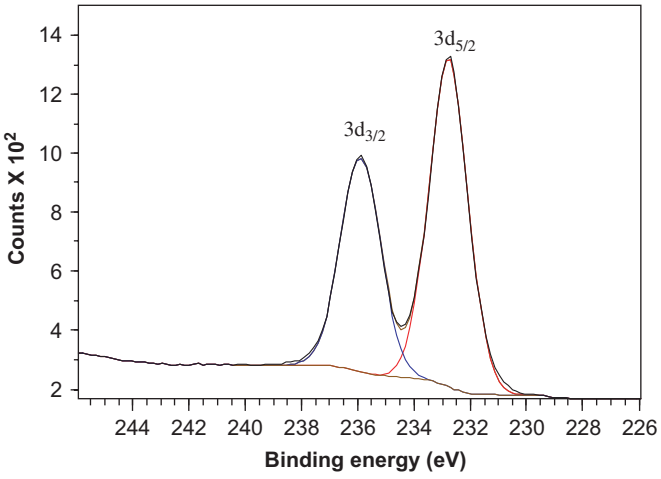

Fig. 8. Mo 3*d* XPS spectrum of the pure $Nb_2Mo_3O_{14}$ oxide.

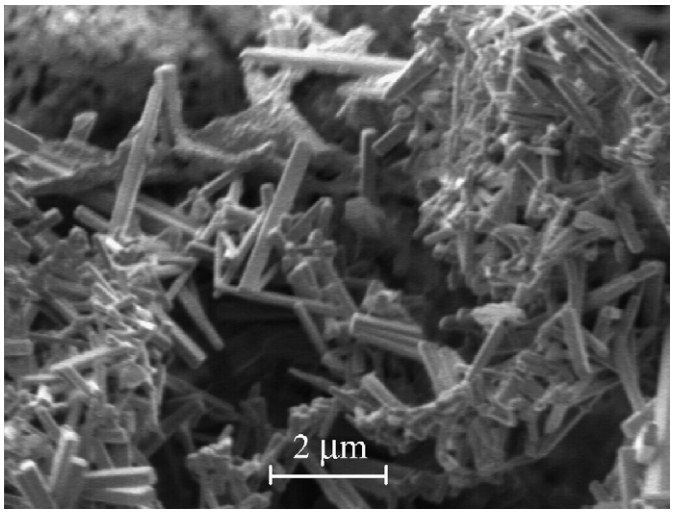

Fig. 9. SEM image of pure $Nb_2Mo_3O_{14}$ oxide.

As for the Nb–Ta oxides, SEM was implemented to study the morphology of the sample (Fig. 9). On the SEM images, the oxide exhibits a quite regular shape and elongated particles. This morphology is quite similar to the morphology of the same oxide prepared by a molecular precursor route while solid-state reaction leads to more sintered particles [12].

3.3.3. *Nb–V–O system*

A hybrid material based on Nb and V was used in order to prepare the multimetallic oxide $NbVO_5$. Calcination of the precursor at 500 °C leads to the formation of Nb-rich phases, namely Nb_9VO_{25} (JCPDS file 49-0289) and $Nb_{18}V_4O_{55}$ (JCPDS file 46-0087), and one V-rich phase, namely V_2O_5 (JCPDS file 41-1426). When the temperature is raised to 600 °C, the relative amount of the oxide $Nb_{18}V_4O_{55}$ decreases while the amount of the phase Nb_9VO_{25} increases. In these conditions, the simple oxide V_2O_5 is still present. The formation of a mixture of different phases is not surprising as the mixed oxide $NbVO_5$ has been synthesised up to now only by a sol–gel method described by Amarilla et al. [25]. Further investigations are required in order to search for some conditions leading to the pure phase $NbVO_5$.

4. Conclusions

Homogeneous hybrid organic–inorganic materials based on group 5 elements have been prepared successfully and used as precursors for group 5 multimetallic oxides. The synthesis of single phase compounds has been confirmed by XRD for the Nb–Ta–O and Nb–Mo–O systems. In particular, the hybrid organic–inorganic precursor method has allowed the formation of a solid solution $(Nb_{1-x}Ta_x)_2O_5$ which was evidenced by a regular evolution of the lattice parameter *c* as a function of the Ta^V amount. Optimised conditions for the synthesis of the mixed oxide $Nb_2Mo_3O_{14}$ were determined by calcination of the precursor at 350 °C followed by a second step of calcination at 700 °C. In the Nb–V–O system, calcination of the precursors at 500 and 600 °C led to a mixture of different Nb-rich phases together with V_2O_5. Moreover, the morphology of the samples has been studied by SEM. A disordered porous character was observed for the Nb–Ta oxides and highly regular shape particles for the Nb–Mo oxide.

Acknowledgments

The authors thank the Belgian National Fund for Scientific Research (FNRS) for the financial support, the CBMM Company (Brazil) for supplying niobic acid and Prof. Gaigneaux for access to the XPS facilities. They are also grateful to Professor Laschewsky and Dr. F. Rullens for fruitful discussions. This work has been performed in the frame of the Interuniversity Attraction Poles Programme of the Belgian State, Belgian Science Policy, Project INANOMAT, P6/17.

References

[1] P. Ayyub, M.S. Multani, V.R. Palmkar, R. Vijayaraghavan, Phys. Rev. B 34 (1986) 8137.
[2] T. Okubo, M. Kakihana, J Alloys Compd. 256 (1997) 151.
[3] R.H.H. Smits, K. Seshan, J.R.H. Ross, J. Phys. Chem. 99 (1995) 9169.
[4] P. Moggi, M. Devillers, P. Ruiz, G. Predieri, D. Cauzzi, S. Morselli, O. Ligabue, Catal. Today 81 (2003) 77.
[5] J.N. Kondo, T. Yamashita, T. Katou, B. Lee, D. Lu, M. Hara, K. Domen, Stud. Surf. Sci. Catal. 141 (2002) 265.
[6] Z.G. Zou, H. Arakawa, J.H. Ye, J. Mater. Res. 17 (2002) 1446.
[7] D. Bayot, B. Tinant, M. Devillers, Catal. Today 78 (2003) 439.
[8] V.K. Trunov, L.M. Kovba, E.I. Sirotkina, Dokl. Akad. Nauk. SSSR 153 (1963) 1085.
[9] G.P. Mohanty, L.J. Fiegel, J.H. Healy, J. Phys. Chem. 68 (1964) 208.
[10] J.A. Schwarz, Chem. Rev. 95 (1995) 477.
[11] B. Lee, T. Yamashita, D.L. Lu, J.N. Kondo, K. Domen, Chem. Mater. 14 (2002) 867.
[12] D. Bayot, M. Devillers, Inorg. Chem. 45 (2006) 4407.
[13] D. Bayot, M. Devillers, Chem. Mater. 16 (2004) 5401.

[14] P. Köberle, A. Laschewsky, T.D. Lomax, Makromol. Chem. Rapid Commun. 12 (1991) 427.
[15] P. Köberle, A. Laschewsky, B. Mayer, V. Vermylen, Macromolecules 27 (1994) 2165.
[16] P. Favresse, A. Laschewsky, Macromol. Chem. Phys. 200 (1999) 887.
[17] P. Köberle, A. Laschewsky, Macromol. Symp. 88 (1994) 165.
[18] F. Rullens, N. Deligne, A. Laschewsky, M. Devillers, J. Mater. Chem. 15 (2005) 1668.
[19] F. Rullens, A. Laschewsky, M. Devillers, Chem. Mater. 18 (2006) 771.
[20] F. Rullens, M. Devillers, A. Laschewsky, J. Mater. Chem. 14 (2004) 3421.
[21] F. Rullens, M. Devillers, A. Laschewsky, Macromol. Chem. Phys. 205 (2004) 1155.
[22] D. Bayot, B. Tinant, B. Mathieu, J.-P. Declercq, M. Devillers, Eur. J. Inorg. Chem. (2003) 737.
[23] D. Bayot, B. Tinant, M. Devillers, Inorg. Chem. 43 (2004) 5999.
[24] D. Bayot, M. Degand, M. Devillers, J. Solid State Chem. 178 (2005) 2635.
[25] J.M. Amarilla, B. Casal, E. Ruiz-Hitzky, J. Solid State Chem. 99 (1992) 258.